

# REPORT DOCUMENTATION PAGE

*Form Approved*  
OMB No. 0704-0188

Public reporting burden for this collection of information is estimated to average 1 hour per response, including the time for reviewing instructions, searching existing data sources, gathering and maintaining the data needed, and completing and reviewing this collection of information. Send comments regarding this burden estimate or any other aspect of this collection of information, including suggestions for reducing this burden to Department of Defense, Washington Headquarters Services, Directorate for Information Operations and Reports (0704-0188), 1215 Jefferson Davis Highway, Suite 1204, Arlington, VA 22202-4302. Respondents should be aware that notwithstanding any other provision of law, no person shall be subject to any penalty for failing to comply with a collection of information if it does not display a currently valid OMB control number. **PLEASE DO NOT RETURN YOUR FORM TO THE ABOVE ADDRESS.**

<b>1. REPORT DATE (DD-MM-YYYY)</b> 23-11-2009		<b>2. REPORT TYPE</b> Journal Article		<b>3. DATES COVERED (From - To)</b>	
<b>4. TITLE AND SUBTITLE</b>  Synthesis and Properties of N <sub>7</sub> O <sup>+</sup> (PREPRINT)				<b>5a. CONTRACT NUMBER</b>	
				<b>5b. GRANT NUMBER</b>	
				<b>5c. PROGRAM ELEMENT NUMBER</b>	
<b>6. AUTHOR(S)</b> Karl O. Christe, Ralf Haiges, and William W. Wilson (USC); Jerry A. Boatz(AFRL/RZSP)				<b>5d. PROJECT NUMBER</b>	
				<b>5e. TASK NUMBER</b>	
				<b>5f. WORK UNIT NUMBER</b> 50260541	
<b>7. PERFORMING ORGANIZATION NAME(S) AND ADDRESS(ES)</b>  Air Force Research Laboratory (AFMC) AFRL/RZSP 10 E. Saturn Blvd. Edwards AFB CA 93524-7680				<b>8. PERFORMING ORGANIZATION REPORT NUMBER</b>  AFRL-RZ-ED-JA-2009-413	
<b>9. SPONSORING / MONITORING AGENCY NAME(S) AND ADDRESS(ES)</b>  Air Force Research Laboratory (AFMC) AFRL/RZS 5 Pollux Drive Edwards AFB CA 93524-7048				<b>10. SPONSOR/MONITOR'S ACRONYM(S)</b>	
				<b>11. SPONSOR/MONITOR'S NUMBER(S)</b> AFRL-RZ-ED-JA-2009-413	
<b>12. DISTRIBUTION / AVAILABILITY STATEMENT</b>  Approved for public release; distribution unlimited (PA #09507).					
<b>13. SUPPLEMENTARY NOTES</b> For the Journal of Inorganic Chemistry					
<b>14. ABSTRACT</b> The reaction of NOF <sub>2</sub> +SbF <sub>6</sub> <sup>-</sup> with an equimolar amount of HN <sub>3</sub> in anhydrous HF solution at -45 °C produces N <sub>3</sub> NOF+SbF <sub>6</sub> <sup>-</sup> . When an excess of HN <sub>3</sub> is used in this reaction, N <sub>7</sub> O+SbF <sub>6</sub> <sup>-</sup> is formed. However, this compound could not be isolated as a solid and rapidly decomposed in a quantitative manner with N <sub>2</sub> O evolution to N <sub>5</sub> +SbF <sub>6</sub> <sup>-</sup> . This reaction represents a novel and more convenient synthesis for N <sub>5</sub> +SbF <sub>6</sub> <sup>-</sup> because NOF <sub>2</sub> +SbF <sub>6</sub> <sup>-</sup> is more readily accessible than N <sub>2</sub> F+SbF <sub>6</sub> <sup>-</sup> and the N <sub>5</sub> <sup>+</sup> can be labeled in all five positions with <sup>15</sup> N by the simple use of terminally singly-labeled N <sub>3</sub> <sup>-</sup> . The formation of the N <sub>7</sub> O <sup>+</sup> cation was established by isotopic labeling experiments and theoretical calculations. It is shown that the addition of a second azido ligand to the same central atom allows attack of the negatively charged N $\alpha$ atom of one ligand by the positively charged N $\gamma$ atom of the second ligand, thereby greatly lowering the activation energy barrier towards decomposition and explaining why geminal di-azides are much less stable than either mono-azides or vicinal di-azides. <b>Keywords:</b> polynitrogen chemistry, heptanitrogen oxide cation, theoretical calculations, activation energy barriers.					
<b>15. SUBJECT TERMS</b>					
<b>16. SECURITY CLASSIFICATION OF:</b>			<b>17. LIMITATION OF ABSTRACT</b>	<b>18. NUMBER OF PAGES</b>	<b>19a. NAME OF RESPONSIBLE PERSON</b>
<b>a. REPORT</b>	<b>b. ABSTRACT</b>	<b>c. THIS PAGE</b>			Wayne Kalliomaa
Unclassified	Unclassified	Unclassified	SAR	20	<b>19b. TELEPHONE NUMBER</b> (include area code) N/A

# Synthesis and Properties of $N_7O^+$ (PREPRINT)

*Karl O. Christe\*<sup>†</sup>, Ralf Haiges<sup>†</sup>, William W. Wilson<sup>†</sup> and Jerry A Boatz<sup>‡</sup>*

<sup>†</sup>Loker Research Institute and Department of Chemistry, University of Southern California, Los Angeles, CA 90089-1661, USA, and <sup>‡</sup>Air Force Research Laboratory, Edwards Air Force Base, CA, 93524 USA.

\* To whom correspondence should be addressed: E-mail: kchriste@usc.edu

**RECEIVED DATE** \_\_\_\_\_

Synthesis and Properties of  $N_7O^+$

Author to whom correspondence should be addressed. E-mail: kchriste@usc.edu.

**ABSTRACT:** The reaction of  $NOF_2^+SbF_6^-$  with an equimolar amount of  $HN_3$  in anhydrous HF solution at  $-45\text{ }^\circ\text{C}$  produces  $N_3NOF^+SbF_6^-$ . When an excess of  $HN_3$  is used in this reaction,  $N_7O^+SbF_6^-$  is formed. However, this compound could not be isolated as a solid and rapidly decomposed in a quantitative manner with  $N_2O$  evolution to  $N_5^+SbF_6^-$ . This reaction represents a novel and more convenient synthesis for  $N_5^+SbF_6^-$  because  $NOF_2^+SbF_6^-$  is more readily accessible than  $N_2F^+SbF_6^-$  and the  $N_5^+$  can be labeled in all five positions with  $^{15}\text{N}$  by the simple use of terminally singly-labeled  $N_3^-$ . The formation of the  $N_7O^+$  cation was established by isotopic labeling experiments and theoretical calculations. It is shown that the addition of a second azido ligand to the same central atom allows attack of the negatively charged N $\alpha$  atom of one ligand by the positively charged N $\gamma$  atom of the second ligand, thereby greatly lowering the activation energy barrier towards decomposition and explaining why geminal di-azides are much less stable than either mono-azides or vicinal di-azides.

**Keywords:** polynitrogen chemistry, heptanitrogen oxide cation, theoretical calculations, activation energy barriers.

## Introduction

An area of particular interest for energetic materials is high-nitrogen chemistry. In high-nitrogen chemistry most of the energy release stems from the fact that N-N single bonds (average bond energy ~159 kJ/mol) and N=N double bonds (average bond energy ~419 kJ/mol) are considerably weaker than one third or two thirds of the N≡N triple bond energy in dinitrogen (bond energy of 946 kJ/mol). Therefore, polynitrogen compounds possess large positive heats of formation and decompose exothermically with the liberation of large amounts of N<sub>2</sub>. The formation of large amounts of N<sub>2</sub> in the decomposition products is highly desirable for applications such as gun propellants where the smoke, flame temperature and the corrosion of the gun barrels are greatly reduced by the N<sub>2</sub>. During the last decade, major breakthroughs in this field have been achieved by the syntheses and identification of several novel ions, the V-shaped N<sub>5</sub><sup>+</sup> cation,<sup>1,2</sup> the N<sub>3</sub>NOF<sup>+</sup> cation both as a *z*- and *e*-isomer,<sup>3</sup> and the *cyclo*-N<sub>5</sub><sup>-</sup> anion.<sup>4</sup> The chemistry of N<sub>5</sub><sup>+</sup> and N<sub>5</sub><sup>-</sup> has been highlighted in a recent review paper.<sup>5</sup> The synthesis and characterization of N<sub>3</sub>NOF<sup>+</sup> has also been described already in detail,<sup>3</sup> and here the synthesis of the N<sub>7</sub>O<sup>+</sup> cation is reported. In particular, the question of why N<sub>7</sub>O<sup>+</sup> is thermally so much less stable than N<sub>3</sub>NOF<sup>+</sup> is addressed, and whether this instability is innate to geminal di-azides.

## Experimental Section

*Caution!* Neat HN<sub>3</sub> is highly explosive and should, whenever possible, be handled only in solution. Anhydrous HF can cause severe burns and contact with the skin must be avoided.

**Materials and Apparatus:** All reactions were carried out in Teflon-FEP ampules that were closed by stainless steel valves. Volatile materials were handled in a stainless steel/Teflon-FEP vacuum line.<sup>6</sup> All reaction vessels and the vacuum line were passivated with ClF<sub>3</sub> prior to use. Nonvolatile materials were handled in the dry argon atmosphere of a glove box.

Raman spectra were recorded in the Teflon reactors in the range 4000–80 cm<sup>-1</sup> on a Bruker Equinox 55 FT-RA spectrophotometer, using a Nd-YAG laser at 1064 nm or a Cary Model 83GT spectrometer

using the 488-nm line of an Ar-ion laser. The  $^{14}\text{N}$  NMR spectra were recorded in anhydrous HF as solvent on a Bruker AMX-500 NMR instrument at 36.13 MHz using a 5 mm broad band probe. Neat  $\text{CH}_3\text{NO}_2$  ( $\delta = 0$  ppm), measured at room temperature, was used as an external standard.

The starting materials,  $\text{NOF}_2^+\text{SbF}_6^-$ <sup>7</sup> and  $\text{HN}_3$ <sup>2</sup> were prepared by literature methods. HF was dried by storage over  $\text{BiF}_5$ <sup>8</sup> or  $\text{TaF}_5$ .

**Reaction of  $\text{NOF}_2^+\text{SbF}_6^-$  with  $\text{HN}_3$ :** In a typical experiment,  $\text{NOF}_2^+\text{SbF}_6^-$  (0.3 mmol) was added to a pre-passivated, thin-walled, 4 mm o.d. FEP ampule, which was closed by a stainless steel valve. On the vacuum line, anhydrous HF (270 mg) was condensed in at  $-196$  °C and the  $\text{NOF}_2^+\text{SbF}_6^-$  was dissolved in the HF at room temperature. The ampule was cooled back to  $-196$  °C, and a mixture of  $\text{HN}_3$  (0.3 or 0.6 mmol) and HF (750 or 1500 mg, respectively) was condensed in. The FEP ampule was heat sealed and warmed to  $-80$  °C. It was then inserted into a standard 5 mm o.d. glass NMR tube and quickly transferred into the probe of the NMR spectrometer. The sample was warmed to ambient temperature in steps of  $10$  °C and monitored by NMR spectroscopy.

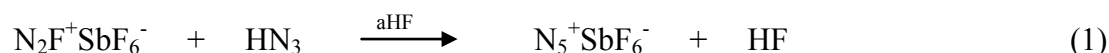
**Theoretical Methods:** The molecular structures, harmonic vibrational frequencies, and infrared and Raman vibrational intensities were calculated using (a) second order perturbation theory (MP2, also known as MBPT(2)<sup>9</sup>) and the 6-311G(2df) basis set,<sup>10</sup> denoted as MP2/6-311G(2df), (b) MP2 with the correlation consistent polarized valence triple-zeta basis set,<sup>11</sup> i.e., MP2/cc-pvtz, and (c) density functional theory methods using the B3LYP hybrid functional,<sup>12</sup> which included the VWN5 correlation functional<sup>13</sup> and the 6-311G(2df) basis set (B3LYP/6-311G(2df)). In addition, the structure and harmonic vibrational frequencies of the  $\text{C}_{2v}$  isomer of  $\text{N}_7\text{O}^+$  were computed using the coupled cluster singles plus doubles with a perturbative estimate of triples (CCSD(T)<sup>14</sup>) method, with the 6-31G(d) basis set.<sup>15</sup> Hessians (energy second derivatives) were calculated for all stationary points to verify them as either local minima or transition states (i.e., having zero or one negative eigenvalue of the Hessian, respectively.) Intrinsic reaction coordinate<sup>16</sup> traces were generated using the Gonzales-Schlegel second-order method.<sup>17</sup> The relative energies of all stationary points were refined by performing “completely renormalized” CR-CCSD(T)<sup>18</sup> single point energy computations at the MP2/6-311G(2df) geometries.

B3LYP/6-311G(2df) (MP2/6-311G(2df)) zero-point vibrational energy corrections were scaled by 0.9806 (0.9748).<sup>19</sup> The calculations were performed using the electronic structure codes GAMESS,<sup>20</sup> Gaussian 03,<sup>21</sup> and ACES II.<sup>22</sup> The second derivatives were analyzed using the program BMATRIX.<sup>23</sup>

## Results and Discussion

### Chemical Synthesis

In the synthesis of  $N_5^+$ ,<sup>1,2</sup>  $N_2F^+$  was reacted with  $HN_3$  to replace the F atom by an azido group (Eq. 1).



A similar approach was applied to the well known  $NOF_2^+$  cation<sup>7,24-29</sup> and, when a stoichiometric amount of  $HN_3$  was used, formation of the  $N_3NOF^+$  cation resulted (Eq. 2).

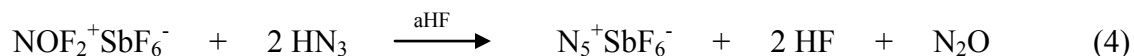


The  $N_3NOF^+SbF_6^-$  salt was found to be marginally stable at ambient temperature<sup>3</sup> and, therefore, an obvious challenge was to explore whether the second F atom could also be replaced by an azido group and, thus, provide a synthesis for the novel  $N_7O^+$  cation (Eq. 3).



Replacement of F by  $N_3$  started to proceed at temperatures as low as  $-64$  °C and, when stoichiometric amounts of  $NOF_2^+SbF_6^-$  and  $HN_3$  were used,  $N_3NOF^+SbF_6^-$  was formed in high yield and could be isolated by pumping off the solvent and gaseous products at low temperature. With an excess of  $HN_3$ , replacement of the second fluorine atom started to occur in the same temperature range, however, the expected  $N_7O^+$  cation could neither be directly observed by low-temperature NMR spectroscopy nor be

isolated in the form of its  $\text{SbF}_6^-$  salt. Instead,  $\text{N}_2\text{O}$  gas evolution and quantitative formation of  $\text{N}_5^+\text{SbF}_6^{2-}$  was observed (Eq. 4).

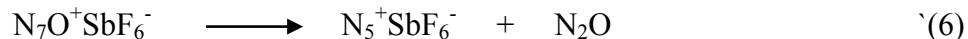


Since the  $\text{NOF}_2^+\text{SbF}_6^-$  is more readily accessible<sup>8</sup> than  $\text{N}_2\text{F}^+\text{SbF}_6^-$ , reaction (4) represents a more convenient and novel synthesis of  $\text{N}_5^+\text{SbF}_6^-$ .

Equations (2) - (4) represent an oversimplification of all the processes occurring in the  $\text{NOF}_2^+/\text{HN}_3/\text{HF}$  system. NMR studies provided evidence for the presence and active participation of several equilibria. For example, at temperatures below  $-43^\circ\text{C}$  in HF solution,  $\text{HN}_3$  can displace  $\text{NOF}_3$  from its  $\text{NOF}_2^+\text{SbF}_6^-$  salt due to the fact that  $\text{H}_2\text{N}_3^+\text{SbF}_6^-$  is practically insoluble in HF at low temperature (Eq. 5).



At  $-43^\circ\text{C}$ , the  $\text{NOF}_3$  is being consumed and  $\text{N}_3\text{NOF}^+$  is formed. It is not clear whether the  $\text{NOF}_3$  or  $\text{NOF}_2^+$  is the reacting species, but generally  $\text{NOF}_2^+$  is much more reactive than  $\text{NOF}_3$ .<sup>7,24-29</sup> At this temperature,  $\text{N}_3\text{NOF}^+$  does not appear to react to an appreciable extent with  $\text{HN}_3$  which, in the HF solution, is present in its protonated form,  $\text{H}_2\text{N}_3^+\text{HF}_2^-(\text{nHF})$ . When the temperature is raised to  $-33^\circ\text{C}$ , the second mole of  $\text{HN}_3$  starts to enter the reaction, all the  $\text{NOF}_3$  is consumed and  $\text{N}_5^+$  and  $\text{N}_2\text{O}$  are formed. Although  $^{15}\text{N}$  labeling experiments (see below) show that the  $\text{N}_5^+$  originates from an intermediate  $\text{N}_7\text{O}^+$ , the  $\text{N}_7\text{O}^+$  is not observable in the NMR spectra, indicating that its decomposition to  $\text{N}_5^+$  and  $\text{N}_2\text{O}$  (Eq. 6) is more rapid than its formation.



It should be pointed out that protonated  $\text{HN}_3$  in HF solution, i.e.,  $\text{H}_2\text{N}_3^+\text{HF}_2^-(\text{nHF})$ , is less reactive towards  $\text{NOF}_2^+$  than is  $\text{HN}_3$ , requiring several days at room temperature to form  $\text{N}_3\text{NOF}^+$ ,  $\text{N}_5^+$  and  $\text{N}_2\text{O}$ . This is not surprising because, due to their positive charges, the two cations should repel each other and not come in close enough contact for entering a reaction. The only reaction taking place would be through their equilibria with the neutral species.

Variation of the solvent (use of  $(\text{CF}_3)_2\text{CFH}$ ) or the azide source (use of  $(\text{CH}_3)_3\text{SiN}_3$ ) did not influence the outcome of these reactions. Obviously, the thermal stability of  $\text{N}_7\text{O}^+$  must be significantly lower than that of  $\text{N}_3\text{NOF}^+$ , thus preempting its direct observation and isolation. Because the  $\text{N}_7\text{O}^+$  cation could not be directly observed, a theoretical study was carried out and its conclusions were experimentally corroborated by isotopic labeling experiments.

### Theoretical Studies

Based on the known structure of  $\text{N}_3\text{NOF}^{+3}$  and the reaction leading to its formation, the most probable structure for  $\text{N}_7\text{O}^+$ , is the  $C_{2v}$  structure shown in Figure 1.

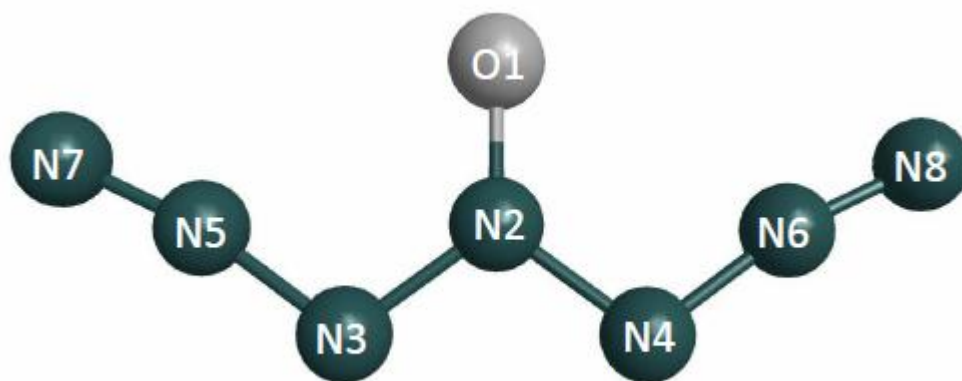


Figure 1. Minimum energy structure (bond distances in Å, angles in deg) of the  $C_{2v}$  isomer of  $\text{N}_7\text{O}^+$  calculated at the MP2/cc-pvtz level with CCSD(T)/6-31G(d) values given in parentheses: O1-N2, 1.216 (1.221); N2-N3, 1.353 (1.371); N3-N5, 1.293 (1.320); N5-N7, 1.130 (1.131); O1-N2-N3, 126.2 (126.3); N2-N3-N5, 107.7 (106.9); N3-N5-N7, 170.6 (168.8); N2-N3-N5-N7, 180.0 (180.0). Weinhold's NBO charges at the PBE1PBE/6-311+G(2df) level: O -0.25; N2 0.46; N3 -0.13; N5 0.23; N7 0.29.

This structure was confirmed as the energy minimum by theoretical calculations at the B3LYP/6-311G(2df), MP2/6-311G(2df), MP2/cc-pvtz, and CCSD(T)/6-31G(d) levels of theory. Other possible

isomers have  $C_s$  and  $C_2$  symmetry and a cyclic  $C_s$  structure (Fig. 2) and are higher in energy than the  $C_{2v}$  structure by 2.6, 17.8 and 27.8 kcal/mol, respectively, at the B3LYP/6-311G(2df) level of theory. The relatively small energy difference of 3 kcal/mol between the  $C_{2v}$  and  $C_s$  structures shows that the  $N_3$  arm in  $N_7O^+$  is quite floppy and can very easily be rotated, an important aspect to remember when potential mechanisms for the  $N_2O$  elimination from  $N_7O^+$  are discussed.

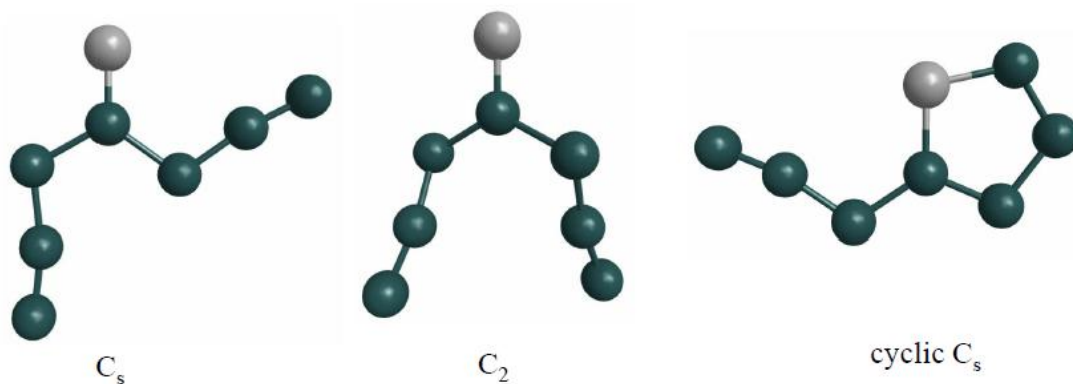


Figure 2. Higher energy, local minima structures for  $N_7O^+$ . Oxygen (nitrogen) atoms are shown as light (dark) circles.

The calculated vibrational frequencies and infrared and Raman intensities are summarized in Table 1. As can be seen from the Table, the calculated frequencies are somewhat method dependent. Since in a catenated species consisting of several nearly linear groups of atoms with identical or similar masses, strong coupling of the vibrational modes must be expected, a normal coordinate analysis was also carried out for  $N_7O^+$  at the B3LYP level. The results from this NCA are summarized in Table 2. The potential energy distribution shows that in most cases the normal vibrations are not highly characteristic and contain contributions from several symmetry coordinates, making many mode descriptions difficult, however, some assignments can be made. The dominant Raman mode,  $\nu_1$ , at  $2314\text{ cm}^{-1}$  and the strong



Table 1 Harmonic vibrational frequencies ( $\text{cm}^{-1}$ ), infrared intensities ( $\text{km/mol}$ ), and Raman intensities [ $\text{\AA}^4/\text{amu}$ ] of  $\text{C}_{2v}\text{N}_7\text{O}^+$

	<b>B3LYP(5)/cc-pvtz</b>	<b>MP2/cc-pvtz</b>	<b>CCSD(T)/6-31G(d)</b>
$a_1$ $\nu_1$	2314 (12) [460]	2194 (9.3) [529]	2234 (6.2)
$\nu_2$	1559 (153) [14]	1630 (85) [31]	1574 (104)
$\nu_3$	1176 (0.4) [12]	1194 (4.7) [29]	1110 (0.3)
$\nu_4$	968 (3.7) [7.6]	995 (1.6) [16.0]	969 (0.3)
$\nu_5$	525 (2.5) [13]	543 (1.0) [17]	503 (3.6)
$\nu_6$	427 (1.9) [2.3]	431 (1.8) [2.0]	411 (0.8)
$\nu_7$	134 (0.01) [6.7]	131 (0.02) [8.3]	129 (0.1)
$a_2$ $\nu_8$	504 (0) [2.0]	475 (0) [1.2]	452 (0)
$\nu_9$	166 (0) [0.2]	161 (0) [0.005]	140 (0)
$b_1$ $\nu_{10}$	703 (9.3) [0.15]	712 (6.3) [0.3]	687 (10)
$\nu_{11}$	540 (6.1) [0.02]	511 (4.1) [0.04]	498 (4.8)
$\nu_{12}$	94 (1.0) [0.08]	97 (1.1) [0.04]	93 (1.8)
$b_2$ $\nu_{13}$	2307 (276) [40]	2182 (383) [61]	2222 (288)
$\nu_{14}$	1220 (1069) [3.1]	1323 (1431) [5.9]	1219 (1281)
$\nu_{15}$	1008 (70) [0.1]	1015 (116) [2.7]	933 (220)
$\nu_{16}$	798 (10) [1.2]	835 (7.4) [1.8]	794 (43)
$\nu_{17}$	495 (0.1) [0.02]	501 (1.4)[0.06]	478 (0.03)
$\nu_{18}$	225 (2.8) [1.5]	221 (1.6) [0.6]	215 (2.8)

IR mode,  $\nu_{13}$ , at  $2307 \text{ cm}^{-1}$  are predominantly due to the in-phase and out-of-phase coupled stretching modes, respectively, of the two terminal N-N bonds. The  $1559 \text{ cm}^{-1}$  vibration,  $\nu_2$ , is 51 % stretching of the N-O bond, and the dominant infrared mode,  $\nu_{14}$ , at  $1220 \text{ cm}^{-1}$  is 60 % due to the rocking motion of

Table 2 B3LYP/cc-pvtz Force Constants<sup>a</sup> and Potential Energy Distribution<sup>b</sup> of C<sub>2v</sub> N<sub>7</sub>O<sup>+</sup>

Symmetry Class	Frequency cm <sup>-1</sup>	Force Constants							PED
		F <sub>11</sub>	F <sub>22</sub>	F <sub>33</sub>	F <sub>44</sub>	F <sub>55</sub>	F <sub>66</sub>	F <sub>77</sub>	
a <sub>1</sub>	2314	21.351	0.182	1.260	-0.478	-0.098	-0.209	0.102	75.1S <sub>1</sub> + 23.8S <sub>3</sub>
	1559		11.249	-0.280	1.674	1.090	0.061	0.019	51.4S <sub>2</sub> + 18.7S <sub>6</sub> + 15.5S <sub>4</sub> + 13.4S <sub>5</sub>
	1176			7.078	0.558	-0.650	1.121	0.261	61.3S <sub>3</sub> + 23.0S <sub>4</sub>
	968				6.048	-1.001	0.881	-0.009	44.9S <sub>6</sub> + 26.4S <sub>7</sub> + 14.2S <sub>4</sub>
	525					4.076	-0.275	-0.037	86.6S <sub>7</sub>
	427						1.710	0.083	79.7S <sub>7</sub> + 16.7S <sub>5</sub>
	133							0.425	66.9S <sub>7</sub> + 28.3S <sub>6</sub>
a <sub>2</sub>	504	F <sub>88</sub> 0.125	F <sub>99</sub> -0.001						98.5S <sub>9</sub>
	166		0.017						76.4S <sub>12</sub> + 23.5S <sub>11</sub>
b <sub>1</sub>	703	F <sub>10,10</sub> 0.785	F <sub>11,11</sub> -0.298	F <sub>12,12</sub> -0.014					55.4S <sub>11</sub> + 44.7S <sub>10</sub>
	540		0.278	0.009					99.1S <sub>12</sub>
	94			0.018					76.4S <sub>12</sub> + 23.5S <sub>11</sub>
b <sub>2</sub>	2307	F <sub>13,13</sub> 21.336	F <sub>14,14</sub> 1.321	F <sub>15,15</sub> -0.504	F <sub>16,16</sub> -0.186	F <sub>17,17</sub> -0.003	F <sub>18,18</sub> 0.106		75.3S <sub>13</sub> + 22.8S <sub>14</sub>
	1220		6.703	0.715	1.017	-0.271	0.273		60.1S <sub>17</sub> + 28.3S <sub>15</sub>
	1008			4.446	0.852	0.451	-0.022		82.0S <sub>14</sub> + 10.5S <sub>17</sub>
	798				1.593	0.060	0.069		43.1S <sub>18</sub> + 36.6S <sub>16</sub> + 10.6S <sub>17</sub>
	495					1.395	-0.005		67.8S <sub>18</sub> + 24.8S <sub>17</sub>
	225						0.419		76.9S <sub>18</sub> + 19.1S <sub>16</sub>

<sup>a</sup> Stretching constants in mdyne/Å, deformation constants in mdyne-Å/rad<sup>2</sup>, and stretch-bend interaction constants in mdyne/rad.

<sup>b</sup> PED in percent. Coordinates contributing less than 10 percent have been omitted. Coordinates have been defined as follows (normalization factors have been omitted): S<sub>1</sub> = ν(N<sub>5</sub>-N<sub>7</sub>)+ν(N<sub>6</sub>-N<sub>8</sub>), S<sub>2</sub> = ν(O-N<sub>2</sub>), S<sub>3</sub> = ν(N<sub>3</sub>-N<sub>5</sub>)+ν(N<sub>4</sub>-N<sub>6</sub>), S<sub>4</sub> = ν(N<sub>2</sub>-N<sub>3</sub>)+ν(N<sub>2</sub>-N<sub>4</sub>), S<sub>5</sub> = δ(O-N<sub>2</sub>-N<sub>3</sub>)+δ(O-N<sub>2</sub>-N<sub>4</sub>), S<sub>6</sub> = δ(N<sub>2</sub>-N<sub>3</sub>-N<sub>5</sub>)+δ(N<sub>2</sub>-N<sub>4</sub>-N<sub>6</sub>), S<sub>7</sub> = δ(N<sub>3</sub>-N<sub>5</sub>-N<sub>7</sub>)+δ(N<sub>4</sub>-N<sub>6</sub>-N<sub>8</sub>), S<sub>8</sub> = ω(O-N<sub>2</sub>-N<sub>3</sub>-N<sub>5</sub>)+ω(O-N<sub>2</sub>-N<sub>4</sub>-N<sub>6</sub>), S<sub>9</sub> = ω(N<sub>2</sub>-N<sub>3</sub>-N<sub>5</sub>-N<sub>7</sub>)+ω(N<sub>2</sub>-N<sub>4</sub>-N<sub>6</sub>-N<sub>8</sub>), S<sub>10</sub> = ω(O-N<sub>2</sub>-N<sub>3</sub>-N<sub>4</sub>), S<sub>11</sub> = ω(O-N<sub>2</sub>-N<sub>3</sub>-N<sub>5</sub>)-ω(O-N<sub>2</sub>-N<sub>4</sub>-N<sub>6</sub>), S<sub>12</sub> = ω(N<sub>2</sub>-N<sub>3</sub>-N<sub>5</sub>-N<sub>7</sub>)-ω(N<sub>2</sub>-N<sub>4</sub>-N<sub>6</sub>-N<sub>8</sub>), S<sub>13</sub> = ν(N<sub>5</sub>-N<sub>7</sub>)-ν(N<sub>6</sub>-N<sub>8</sub>), S<sub>14</sub> = ν(N<sub>3</sub>-N<sub>5</sub>)-ν(N<sub>4</sub>-N<sub>6</sub>), S<sub>15</sub> = ν(N<sub>2</sub>-N<sub>3</sub>)-ν(N<sub>2</sub>-N<sub>4</sub>), S<sub>16</sub> = δ(N<sub>2</sub>-N<sub>3</sub>-N<sub>5</sub>)-δ(N<sub>2</sub>-N<sub>4</sub>-N<sub>6</sub>), S<sub>17</sub> = δ(O-N<sub>2</sub>-N<sub>3</sub>)-δ(O-N<sub>2</sub>-N<sub>4</sub>), S<sub>18</sub> = δ(N<sub>3</sub>-N<sub>5</sub>-N<sub>7</sub>)-δ(N<sub>4</sub>-N<sub>6</sub>-N<sub>8</sub>)

the oxygen atom. The isotopic shifts which should be observed in the vibrational spectra upon replacement of  $^{16}\text{O}$  by  $^{18}\text{O}$  and of all  $^{14}\text{N}$ s by  $^{15}\text{N}$ s have also been calculated. The results are summarized in Table 3.

Table 3  $^{18}\text{O}$  and  $^{15}\text{N}$  Isotopic Shifts ( $\text{cm}^{-1}$ ) of  $\text{C}_{2v} \text{N}_7\text{O}^+$  at the B3LYP/cc-pvtz level

$^{16}\text{O}-^{14}\text{N}$	$^{18}\text{O}-^{14}\text{N}$	$^{16}\text{O}-^{15}\text{N}$	$^{18}\text{O}-^{15}\text{N}$	$(^{18}\text{O}-^{14}\text{N}) - (^{16}\text{O}-^{14}\text{N})$	$(^{16}\text{O}-^{15}\text{N}) - (^{16}\text{O}-^{14}\text{N})$	$(^{18}\text{O}-^{15}\text{N}) - (^{16}\text{O}-^{14}\text{N})$
2314.0	2314.0	2235.6	2235.6	0.0	-78.4	-78.4
2307.7	2307.7	2229.5	2229.5	0.0	-78.2	-78.2
1558.9	1525.9	1526.9	1492.3	-33.0	-32.0	-66.6
1220.2	1218.2	1180.1	1178.0	-2.0	-40.1	-42.2
1176.2	1175.2	1136.9	1135.9	-1.0	-39.3	-40.3
1007.9	1007.4	974.0	973.5	-0.5	-33.9	-34.4
968.0	955.1	942.2	930.1	-12.9	-25.8	-37.9
798.1	795.4	772.7	769.9	-2.7	-25.4	-28.2
703.2	698.9	682.0	677.6	-4.3	-21.2	-25.6
539.6	539.5	521.3	521.2	-0.1	-18.3	-18.4
525.2	524.7	507.8	507.2	-0.5	-17.4	-18.0
504.5	504.5	487.4	487.4	0.0	-17.1	-17.1
494.9	483.7	484.8	473.5	-11.2	-10.1	-21.4
427.4	424.0	414.7	411.6	-3.4	-12.7	-15.8
225.3	221.1	220.1	216.0	-4.2	-5.2	-9.3
166.4	166.4	160.8	160.8	0.0	-5.6	-5.6
133.9	133.1	129.7	129.0	-0.8	-4.2	-4.9
93.7	92.3	91.4	90.0	-1.4	-2.3	-3.7

Finally, the nitrogen NMR shifts have also been calculated for  $N_7O^+$  at the PBE1BPE/6-311+G(2df) level of theory. The following chemical shifts in ppm relative to  $CH_3NO_2$  are predicted:  $N_2 = -10.2$ ,  $N_3 = -157.9$ ,  $N_5 = -164.0$ ,  $N_7 = -64.8$ . These data will facilitate future experimental searches for this interesting cation.

Since all attempts to isolate  $N_7O^+$  had been unsuccessful, while  $N_3NOF^+$  possesses good thermal stability, the question arose whether this was due to a poor choice of reagents or reaction conditions or if there is a general innate stability problem with geminal di-azides. In order to deal with this problem, it is imperative to understand the decomposition mechanism of  $N_7O^+$  and *gem*-di-azides in general.

In the study of the decomposition of  $N_7O^+$ , five different pathways were found with transition states (TS), which are illustrated in Figure 3 and with relative energies summarized in Figure 4. Intrinsic reaction coordinate (IRC) calculations were performed to trace the minimum energy pathway from each transition state to reactants and products. Two of the five transition states originate from the  $C_{2v}$  ground state and involve the interaction of the negatively charged oxygen atom with either a positively charged  $N\beta$  atom of an azido group, resulting in a four-membered ring (TS 1), or an also positively charged  $N\gamma$  atom resulting in a five-membered ring (TS 2). (The NBO charge distributions of  $N_7O^+$  are given in the diagram caption of Figure 1.) Note that in case of TS 2, the decomposition pathway is actually a two-step process that goes through a cyclic intermediate I2, which is the same as the cyclic structure shown in Figure 2. The transition state structures preceding (TS2a) and following (TS2b) formation of I2 are nearly identical in structure and relative energy, and therefore only TS2b is shown in Figure 3.

Since the energy difference between the  $C_{2v}$  and the  $C_s$  structure is only  $\sim 3$  kcal/mol with a low interconversion barrier of  $\sim 14$  kcal/mol, a possible decomposition mechanism starting from the  $C_s$  state was also explored. Again, there can be an interaction between the O atom with either  $N\beta$  (TS 4) or  $N\gamma$  (TS 5) of that azido group which points in the same direction as the oxygen. Similar to

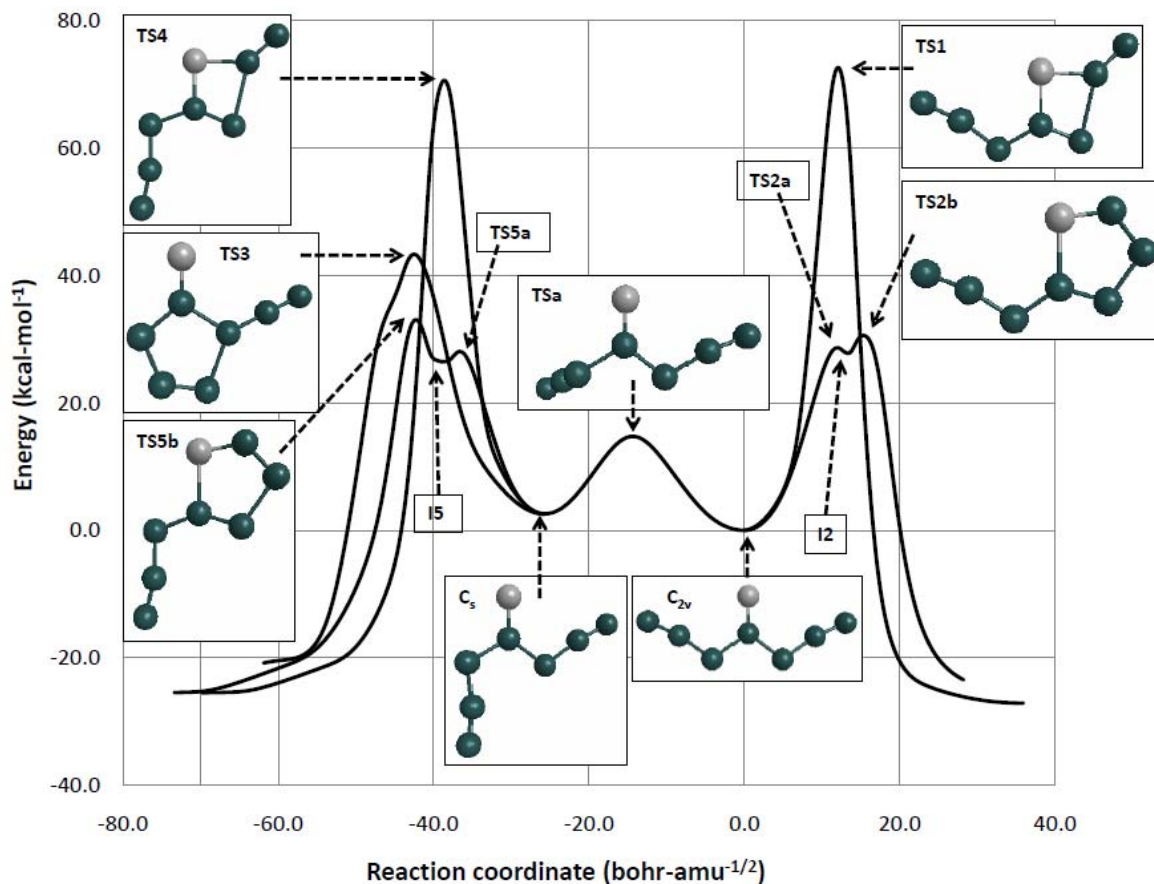


Figure 3. B3LYP/6-311G(2df) intrinsic reaction coordinate traces (solid curves) and stationary points for the decomposition reaction of  $N_7O^+$ . Oxygen (nitrogen) atoms are shown as light (dark) circles. Local minimum I2 is identical to the cyclic isomer shown in Figure 2.

the TS 2 reaction pathway discussed previously, the TS 5 decomposition pathway is actually a two-step process going through a cyclic intermediate I5, preceded and followed by TS5a and TS5b, respectively. The TS5a, TS5b, and I5 stationary points are nearly identical in structure and relative energy, and therefore only TS5b is illustrated in Figure 3. An additional decomposition pathway involves the interaction between the positively charged  $N_\gamma$  atom of the azido group pointing away from the oxygen atom with the negatively charged  $N_\alpha$  atom of the azido group pointing in the same direction as the oxygen atom (TS 3). The calculated barriers are shown in Figures 3 and 4. As can be seen, the barriers involving four-membered cyclic transition states are  $\sim 70$  kcal/mol and are much higher than those involving five-membered rings and, therefore, can be discounted.

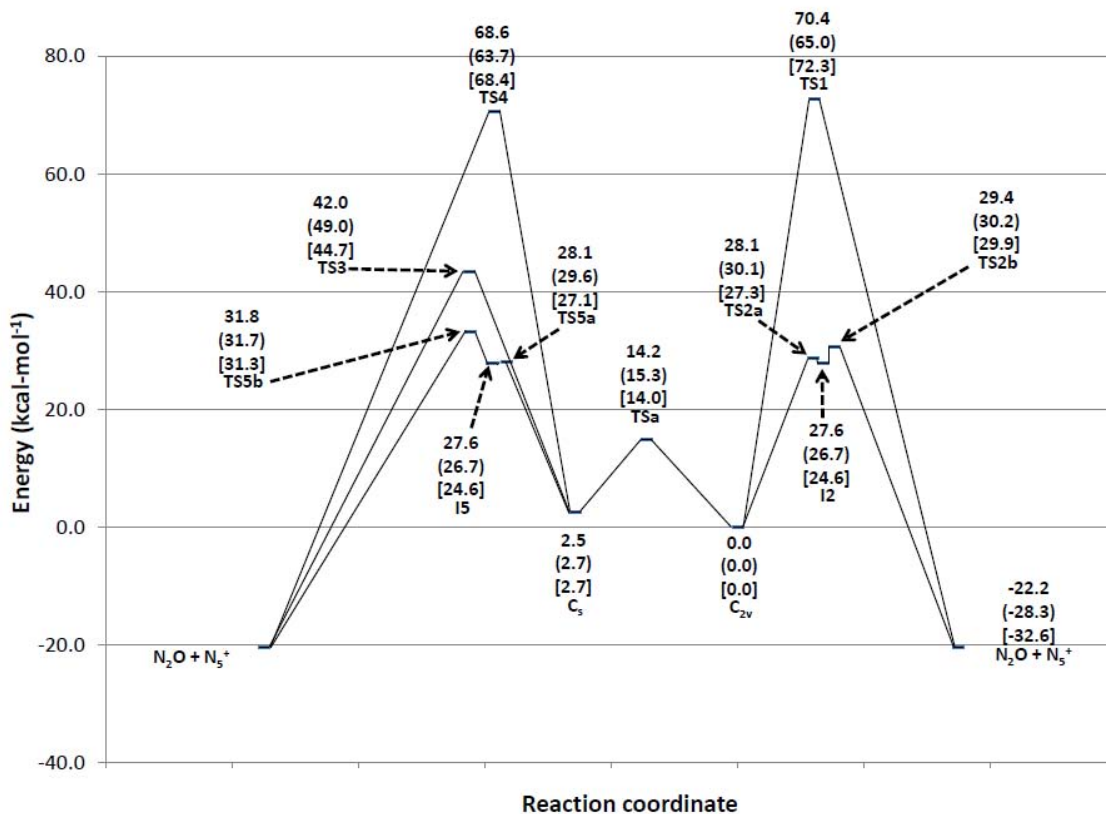


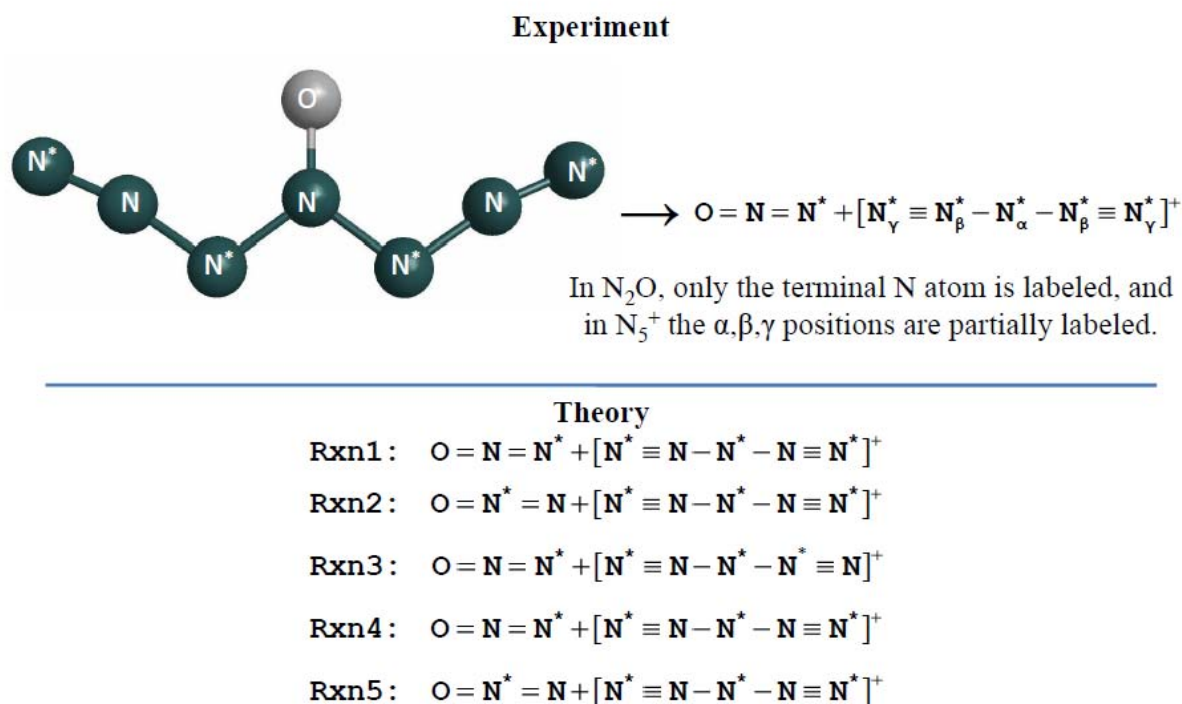
Figure 4. Relative energies (kcal/mol), at the B3LYP/6-311G(2df) level of theory, including scaled B3LYP zero point vibrational energy corrections. MP2/6-311G(2df) and CR-CCSD(T)/cc-pvtz//MP2/6-311G(2df) values, both of which include scaled MP2 zero point vibrational energies, are shown in parentheses and brackets, respectively.

To further discriminate between the different decomposition mechanisms, decomposition studies have been carried out using <sup>15</sup>N labels. For this purpose, labeled  $N_7O^+$  with partial <sup>15</sup>N labels in the  $N_\alpha$  and the  $N_\gamma$  positions were prepared, using singly, terminally labeled azide ion as the starting material (Eq. 7).



The distribution of the <sup>15</sup>N labels in the  $N_7O^+$  decomposition products was determined by <sup>15</sup>N NMR spectroscopy. It was found that the  $N_2O$  was exclusively labeled on the terminal N, i.e.,  $^*N-N-O$ , and that in  $N_5^+$  the <sup>15</sup>N label was equally distributed over all five positions. Of the five different mechanisms that were studied, only the mechanism TS 3 involving the attack of the positively charged  $N_\gamma$  atom of

the azido group pointing away from the oxygen atom on the negatively charged  $N_{\alpha}$  atom of the azido group pointing in the same direction as the oxygen atom can account for the observed distribution of the  $^{15}\text{N}$  labels (Fig. 5) and has a reasonably low activation barrier ( $\sim 42$  kcal/mol) which is about half



Only Rxn 3 predicts the correct label for  $\text{N}_2\text{O}$  and formation of  $[\text{N}_5]^+$  with partial isotopic labels at the  $\alpha, \beta,$  and  $\gamma$  positions.

Figure 5. Comparison of the theoretically predicted and the experimentally found  $^{15}\text{N}$  labels in the decomposition products of  $\text{N}_7\text{O}^+$ .

of that predicted for  $\text{N}_3\text{NOF}^+$  ( $\sim 80$  kcal/mol). Although all of these barriers are higher than expected, it is possible that the calculations overestimate the size of the barriers and/or that the barriers in solution are considerably lower than in the free gas phase. Nevertheless, this study clearly demonstrates that the di-azido  $\text{N}_7\text{O}^+$  cation has a much lower barrier than the mono-azido  $\text{N}_3\text{NOF}^+$  cation, in excellent agreement with the experimental observations. Furthermore, the fact that the preferred mechanism requires the presence of two geminal azido ligands explains the general observation in azide chemistry

that geminal diazides are much more sensitive and unstable than either mono-azides or vicinal di-azides. The inadvertent formation of geminal di-azides as a by product in the synthesis of mono-azides has led in the past to severe accidents and injuries and must be avoided under all circumstances. These conditions apply not only to azide substituted amine oxides, but are equally valid for azidamines and other similar compounds, the only difference being the nature of the elimination product. In the case of multiply azide substituted amines, the elimination product becomes  $N_2$  instead of  $N_2O$ , but the decomposition mechanism remains the same.

### **Conclusions**

The  $N_7O^+$  cation was prepared from the low-temperature reaction of  $NOF_2^+$  with a twofold excess of  $HN_3$  in anhydrous HF solution. The  $N_7O^+$  cation is thermally very unstable and decomposes instantaneously to  $N_5^+$  and  $N_2O$ , thus preventing its direct observation. However, its formation was well established by NMR spectroscopy of the decomposition products, by the use of  $^{15}N$  labeling and by the results from a theoretical study. The decomposition mechanism of  $N_7O^+$  was analyzed and involves the electrophilic attack of the terminal gamma-N atom of one azide ligand on the electron rich alpha-N atom of the second azide ligand, thus explaining the generally observed instability of geminal di-azides.

### **Acknowledgements**

This work was funded by the Air Force Office of Scientific Research, the Office of Naval Research, the Defense Threat Reduction Agency, and the National Science Foundation. Any opinions, findings, and conclusions or recommendations expressed in this material are those of the authors and do not necessarily reflect the views of the National Science Foundation.



## References

- (1) Christe, K. O., Wilson, W. W., Sheehy, J. A., Boatz, J. A., *Angew. Chem. Int. Ed.* **1999**, *38*, 2004.
- (2) Vij, A., Wilson, W. W., Vij, V., Tham, F. S., Sheehy, J. A., Christe, K. O., *J. Am. Chem. Soc.* **2001**, *123*, 6308.
- (3) Wilson, W. W., Haiges, R., Boatz, J. A., Christe, K. O., *Angew. Chem. Int. Ed.* **2007**, *46*, 3023.
- (4) Vij, A., Pavlovich, J. G., Wilson, W. W., Vij, V., Christe, K. O., *Angew. Chem. Int. Ed.* **2002**, *41*, 3051.
- (5) Christe, K. O., *Prop., Explos., Pyrotech.* **2007**, *32*, 194.
- (6) Christe, K. O., Wilson, W. W., Schack, C. J., Wilson, R. D., *Inorg. Synth.* **1986**, *24*, 39.
- (7) Christe, K. O., *J. Am. Chem. Soc.* **1995**, *117*, 6136.
- (8) Christe, K. O., Wilson, W. W., Schack, C. J., *J. Fluorine. Chem.* **1978**, *11*, 71.
- (9) Moller, C., Plesset, M. S., *Phys. Rev.* **1934**, *46*, 618; Pople, J. A., Binkley, J. S., Seeger, R., *Int. J. Quantum Chem.* **1976**, *S10*, 1; Frisch, M. J., Head-Gordon, M., Pople, J. A., *Chem. Phys. Lett.* **1990**, *166*, 275; Bartlett, J., Silver, D. M., *Int. J. Quantum Chem. Symp.* **1975**, *9*, 1927.
- (10) Krishnan, R., Binkley, J. S., Seeger, Pople, J. A., *J. Chem. Phys.* **1980**, *72*, 650; Frisch, M. J., Pople, J. A., Binkley, J. S., *J. Chem. Phys.* **1984**, *80*, 3265.
- (11) Dunning, Jr. T. H., *J. Chem. Phys.* **1989**, *90*, 1007.
- (12) Becke, A. D., *J. Chem. Phys.* **1993**, *98*, 5648; Stephens, P. J., Devlin, F. J., Chablowski, C. F., Frisch, M. J., *J. Phys. Chem.* **1994**, *98*, 11623; Hertwig, R. H., Koch, W., *Chem. Phys. Lett.* **1997**, *268*, 345.
- (13) Vosko, S. H., Wilk, L., Nusair, M., *Can. J. Phys.* **1980**, *58*, 1200.

- (14) Purvis, G. D. III, Bartlett, R. J., *J. Chem. Phys.* **1982**, *76*, 1910.
- (15) Hehre, W. J., Ditchfield, R., Pople, J. A., *J. Chem. Phys.* **1972**, *56*, 2257; Hariharan, P. C., Pople, J. A., *Theoret.Chim.Acta* **1973**, *28*, 213.
- (16) Ishida, K., Morokuma, K., Komornicki, A., *J. Chem. Phys.* **1977**, *66*, 2153.
- (17) Gonzales, C., Schlegel, H. B., *J. Chem. Phys.* **1989**, *90*, 2154.
- (18) Piecuch, P., Kucharski, S. A., Kowalski, K., Musial, M., *Comp. Phys. Commun.* **2002**, *149*, 71; Kowalski, K., Piecuch, P., *J. Chem. Phys.* **2000**, *113*, 18; Kowalski, K., Piecuch, P., *J. Chem. Phys.*, **2000**, *113*, 5644.
- (19) Scott, A. P., Radom, L., *J. Phys. Chem.* **1996**, *100*, 16502.
- (20) a) Schmidt, M. W., Baldridge, K. K., Boatz, J. A., Elbert, S. T., Gordon, M. S., Jensen, J. H., Koseki, S., Matsunaga, N., Nguyen, K. A., Su, S. J., Windus, T. L., Dupuis, M., Montgomery, J. A., *J. Comput. Chem.* **1993**, *14*, 1347; b) Gordon, M. S., Schmidt, M. W.; pp. 1167-1189, in "Theory and Applications of Computational Chemistry: the first forty years" C.E.Dykstra, G.Frenking, K.S.Kim, G.E.Scuseria (editors), Elsevier, Amsterdam, 2005.
- (21) Gaussian 03, Revision D.01, M. J. Frisch, G. W. Trucks, H. B. Schlegel, G. E. Scuseria, M. A. Robb, J. R. Cheeseman, J. A. Montgomery, Jr., T. Vreven, K. N. Kudin, J. C. Burant, J. M. Millam, S. S. Iyengar, J. Tomasi, V. Barone, B. Mennucci, M. Cossi, G. Scalmani, N. Rega, G. A. Petersson, H. Nakatsuji, M. Hada, M. Ehara, K. Toyota, R. Fukuda, J. Hasegawa, M. Ishida, T. Nakajima, Y. Honda, O. Kitao, H. Nakai, M. Klene, X. Li, J. E. Knox, H. P. Hratchian, J. B. Cross, V. Bakken, C. Adamo, J. Jaramillo, R. Gomperts, R. E. Stratmann, O. Yazyev, A. J. Austin, R. Cammi, C. Pomelli, J. W. Ochterski, P. Y. Ayala, K. Morokuma, G. A. Voth, P. Salvador, J. J. Dannenberg, V. G. Zakrzewski, S. Dapprich, A. D. Daniels, M. C. Strain, O. Farkas, D. K. Malick, A. D. Rabuck, K. Raghavachari, J. B. Foresman, J. V. Ortiz, Q. Cui, A. G. Baboul, S. Clifford, J. Cioslowski, B. B. Stefanov, G. Liu, A. Liashenko, P. Piskorz, I. Komaromi, R. L. Martin, D. J. Fox, T. Keith, M. A. Al-Laham, C. Y. Peng, A.

Nanayakkara, M. Challacombe, P. M. W. Gill, B. Johnson, W. Chen, M. W. Wong, C. Gonzalez, and J. A. Pople, Gaussian, Inc., Wallingford CT, 2004.

(22) Stanton, J. F., Gauss, J., Watts, J. D., Nooijen, M., Oliphant, N., Perera, S. A., Szalay, P. G., Lauderdale, W. J., Gwaltney, S. R., Beck, S., Balkova, A., Bernholdt, D. E., Baeck, K. K., Rozyczko, P., Sekino, H., Hober, C., Bartlett, R. J., *ACES II, Quantum Theory Project*; University of Florida: Integral packages included are VMOL (Almlof, J., Taylor, P. R.), BPROPS (Taylor, P. R.), and ABACUS (Helgaker, T., Jensen, H. J. Aa, Jorgensen, P., Olsen, J., Taylor, P. R.).

(23) Komornicki, A., *BMATRIX Version 2.0*; Polyatomics Research Institute: Palo Alto, CA, **1996**.

(24) Fox, W. B., MacKenzie, J. S., Vanderkooi, N., Sukorkik, B., Wamser, C. A., Holmes, J. R., Eibeck, R. E., Stewart, B. B., *J. Am. Chem. Soc.* **1966**, *88*, 2604.

(25) Christe, K. O., Maya, W., *Inorg. Chem.* **1969**, *8*, 1253.

(26) Wamser, C. A., Fox, W. B., Sukornik, B., Holmes, J. R., Stewart, B. B., Juurick, R., Vanderkooi, N., Gould, D., *Inorg. Chem.* **1969**, *8*, 1249.

(27) Christe, K. O., Hon, J. F., Pilipovich, D., *Inorg. Chem.* **1973**, *12*, 84.

(28) Mason, J., Christe, K. O., *Inorg. Chem.* **1983**, *22*, 1849.

(29) Vij, A., Zhang, X., Christe, K. O., *Inorg. Chem.* **2001**, *40*, 416.

## Synopsis

The reaction of  $\text{NOF}_2^+$  with two moles of  $\text{HN}_3$  produces the novel  $\text{N}_7\text{O}^+$  cation which rapidly decomposes to  $\text{N}_5^+$  and  $\text{N}_2\text{O}$  in a quantitative manner. Isotopic labeling elucidates the decomposition mechanism of  $\text{N}_7\text{O}^+$  and explains why geminal di-azides are much less stable than either mono-azides or geminal di-azides.

## Synopsis Artwork

